IMPROVED STRUCTURAL DESIGN RULES FOR CIRCULAR HOLLOW SECTIONS

XIN MENG[1] and LEROY GARDNER[2]

[1]*Department of Civil and Environmental Engineering, Imperial College London, United Kingdom.*
E-mail: xin.meng15@imperial.ac.uk
[2]*Department of Civil and Environmental Engineering, Imperial College London, United Kingdom.*
E-mail: leroy.gardner@imperial.ac.uk

The current Eurocode 3 (EC3) cross-section design provisions for circular hollow sections (CHS) are shown to be unduly conservative due primarily to the abrupt switch between the elastic and fully plastic capacities at the Class 2 to 3 boundary and the overly strict local slenderness limits. To address this issue, improved cross-section design rules for CHS are developed in the present study. Finite element models are established, validated and then utilised for parametric studies, where over 1000 numerical data are generated. To improve the accuracy of EC3, new slenderness limits, expressions for effective section properties and a linear transition between the elastic and plastic resistances over the semi-compact range are proposed; these new design rules are due to appear in the upcoming revision to EN 1993-1-1. Through comparisons with existing test data and the generated numerical results, the improved capacity predictions are clearly shown, but there remains scope for further enhancements, particularly in the Class 1 and 4 domains. This further enhancement is sought through a new generalised slenderness-based resistance method (GSRM), developed by means of the continuous strength method (CSM), where new base curves for CHS featuring more relaxed slenderness limits and the influence of stress gradients, and new resistance functions, are developed. The GSRM for CHS is subsequently assessed, where excellent accuracy and consistency in the resistance predictions under all loading scenarios are revealed over the full range of local slendernesses.

Keywords: Circular hollow sections (CHS), continuous strength method (CSM), cross-section design, local slenderness limits, numerical simulation, semi-compact sections.

1 Introduction

Structural circular hollow sections (CHS) are popular among the tubular section family due to their unique aesthetics and favourable structural properties, and have been widely used in construction as columns, bracing members and truss elements. However, it has been revealed in a number of previous studies that the current cross-section design rules for CHS, such as Eurocode 3 (EC3) and the continuous strength method (CSM), are often unduly conservative. This issue is therefore addressed in this paper. Finite element (FE) models of CHS are developed, validated and then utilised for parametric studies to numerically generate cross-section resistance data, as described in Section 2. The development of improved cross-section design rules for EC3 and a new CSM-based design approach for CHS are presented in Sections 4 and 5 respectively. The obtained FE results, along with the previously collected test data, are used for evaluation of the current codified design methods and the proposed design approaches.

Proceedings of the 17th International Symposium on Tubular Structures.
Editors: X.D. Qian and Y.S. Choo

Published by Research Publishing, Singapore.
ISBN: 978-981-11-0745-0; doi:10.3850/978-981-11-0745-0_074-cd

2 Numerical Simulation

Finite element (FE) models to simulate the cross-sectional behaviour of CHS under compression, bending and combined loading are presented in this section. The numerical models were developed and validated against existing test data, as presented in Section 2.1. Parametric studies are then described in Section 2.2, by means of which numerical data over a wider range of cross-section sizes, material properties and load combinations were generated.

2.1 *Development of numerical models*

Geometrically and materially nonlinear analyses with imperfections (GMNIA) were performed using Abaqus (Abaqus 2016) to simulate the cross-sectional behaviour of CHS. The key features of the FE models are described herein. A quarter shell model of CHS with a mesh of element size equal to $0.1\sqrt{(Dt)}$ (where D is the outer diameter and t is the thickness) was established. Symmetry about the mid-length plane and the plane perpendicular to the axis of bending was exploited to improve the computational efficiency. All degrees of freedoms at the end sections were coupled to a reference point, at which suitable boundary conditions were applied. Local geometric imperfections were incorporated into the FE models following the recommendations of Meng and Gardner (submitted). Explicit incorporation of residual stresses was deemed unnecessary for both hot-rolled and cold-formed CHS (Meng and Gardner (submitted)).

The developed FE models were validated against the experimental data reported by Meng and Gardner (2018). The measured stress-strain relationships were used to represent the material behaviour. The statistical results (Table 1) and the comparisons of the load-deformation curves (Figure 1) confirm that the developed models are capable of accurately replicating the test responses of CHS, where $N_{u,FE}$ and $M_{u,FE}$ are the ultimate loads derived from the FE models, $N_{u,test}$ and $M_{u,test}$ are the ultimate loads from the tests and COV is the coefficient of variation. Therefore, the developed FE models are considered suitable for use in parametric studies.

Table 1. Comparisons of cross-section test results with GMNIA results.

Load case	No. of tests	$N_{u,FE}$ / $N_{u,test}$		$M_{u,FE}$ / $M_{u,test}$	
		Mean	COV	Mean	COV
Compression	6	0.984	0.012	-	-
Bending	6	-	-	1.017	0.019
Combined loading	15	0.996	0.015	0.992	0.020

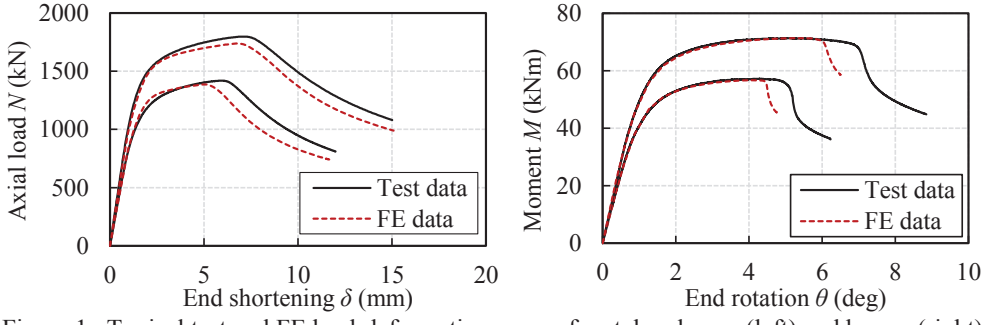

Figure 1. Typical test and FE load-deformation curves for stub columns (left) and beams (right).

2.2 *Parametric studies*

A parametric investigation was conducted using the developed FE models to expand the data pool over a wider spectrum of material grades (S355 to S900), local slendernesses (with D / $t\varepsilon^2$

ranging from 20 to 240, where $\varepsilon^2 = 235 / f_y$ and f_y is the yield strength) and combinations of compression and bending. The stress-strain curves were generated from the predictive models of Yun and Gardner (2017) and Gardner and Yun (2018) for hot-rolled and cold-formed CHS respectively; the input parameters, including the Young's modulus E, yield strength f_y and ultimate strength f_u, were taken as the nominal values specified in EN 1993-1-1:2005. In total, 1078 numerical data were generated from the presented parametric studies.

3 Existing Cross-Section Design Methods

3.1 *Eurocode 3 – EN 1993-1-1:2005*

The current EC3 cross-section design rules for CHS in EN 1993-1-1:2005 are outlined in this section. Cross-section classification is initially performed to account for the susceptibility to local buckling. The slenderness limits of $D/t\varepsilon^2 = 50$ for Class 1, 70 for Class 2 and 90 for Class 3 CHS are adopted in EN 1993-1-1:2005 under all loading conditions.

The cross-section resistance to axial compression $N_{c,Rd}$ is equal to $N_{pl,Rd} = Af_y / \gamma_{M0}$ for Class 1 to 3 and $N_{eff,Rd} = A_{eff}f_y / \gamma_{M0}$ for Class 4 CHS, where A is the cross-sectional area and A_{eff} is the effective area and γ_{M0} is the partial safety factor for cross-section resistance. The cross-section resistance to bending $M_{c,Rd}$ is equal to $M_{pl,Rd} = W_{pl}f_y / \gamma_{M0}$ for Class 1 and 2, $M_{el,Rd} = W_{el}f_y / \gamma_{M0}$ for Class 3 and $M_{eff,Rd} = W_{eff}f_y / \gamma_{M0}$ for Class 4 CHS, where W_{pl}, W_{el} and W_{eff} are the elastic, plastic and effective section moduli respectively. For the case of combined compression and bending, the design interaction formulae are given by Eqs (1-3), where N_{Ed} and M_{Ed} are the design loads.

$$\left(N_{Ed} / N_{pl,Rd}\right)^{1.7} + M_{Ed} / M_{el,Rd} \le 1 \text{ for Class 1 and 2 CHS} \quad (1)$$

$$N_{Ed} / N_{pl,Rd} + M_{Ed} / M_{el,Rd} \le 1 \text{ for Class 3 CHS} \quad (2)$$

$$N_{Ed} / N_{eff,Rd} + M_{Ed} / M_{eff,Rd} \le 1 \text{ for Class 4 CHS} \quad (3)$$

3.2 *Continuous strength method*

The continuous strength method (CSM) is a deformation-based design approach, which provides an alternative treatment to cross-section classification and captures the benefits from strain hardening. The key features of the CSM are described herein. The local slenderness $\overline{\lambda}_c$ is defined as $(f_y / \sigma_{cr})^2$, where σ_{cr} is the elastic critical buckling stress. A base curve describing the relationship between $\overline{\lambda}_c$ and the deformation capacity $\varepsilon_{csm} / \varepsilon_y$ is then employed, where ε_{csm} is the maximum strain at the ultimate load and $\varepsilon_y = f_y / E$ is the yield strain. Unlike the traditional elastic, perfectly plastic material model that is typically used in the current design codes, advanced material models that incorporate the strain hardening range are used in the CSM design. CSM resistance functions for isolated loading have been developed based on the cross-section shape and the material model. The CSM has recently been extended to CHS, and details on the design procedure and design expressions are presented in Buchanan et al. (2016).

4 Improved EC3 Design Rules for CHS

For a Class 3 (semi-compact) CHS, the current EC3 design rules limit the cross-section resistance to its elastic resistance, ignoring any benefit from the partial spread of plasticity. This results in a step in the EC3 design resistance function at the boundary between Class 2 and 3, leading to unduly conservative resistance predictions for pure bending and combined loading. For Class 4 CHS, no guidance on the calculation of effective section properties is provided. New design rules are therefore proposed to improve the current EC3 and are assessed in this section.

4.1 *Design proposal*

More relaxed Class 3 slenderness limits of $D/t\varepsilon^2 = 140$ for bending and $2520/(5\psi + 23)$ for CHS under combined loading have been proposed by Chan and Gardner (2008a), where ψ is the ratio of the minimum stress to the maximum stress over the cross-section depth (with compression positive) assuming an elastic stress distribution. Expressions for A_{eff} (Eq. (4)) and W_{eff} (Eq. (5)) have been developed by Chan and Gardner (2008b) and Chan and Gardner (2008a) respectively for Class 4 CHS.

$$A_{eff} = A\sqrt{\frac{90\varepsilon^2}{D/t}} \quad \text{for } 90 < D/t\varepsilon^2 \le 240 \tag{4}$$

$$W_{eff} = W_{el}\sqrt[4]{\frac{140\varepsilon^2}{D/t}} \quad \text{for } 140 < D/t\varepsilon^2 \le 240 \tag{5}$$

To account for the additional resistance arising from partial plastification, the elasto-plastic section modulus W_{ep}, which is a linear transition between the plastic and elastic section moduli W_{pl} and W_{el} with slenderness, is proposed, as given by Eqs (6-7). New design expressions with W_{ep} adopted in place of W_{el} are subsequently formulated. For the case of bending, the moment resistance is taken as $M_{ep,Rd} = W_{ep}f_y / \gamma_{M0}$, while for compression plus bending, a linear interaction formula incorporating M_{ep} is proposed, as given by Eq. (8). The presented improved design rules are illustrated in Figure 2. The improved design rules for EC3 presented herein have been accepted for incorporation into the upcoming revision of EN 1993-1-1.

$$W_{ep} = W_{pl} - \left(W_{pl} - W_{el}\right)\beta_{ep} \tag{6}$$

$$\beta_{ep} = \max\left(\frac{D/t - 70\varepsilon^2}{70\varepsilon^2}; 0\right) \text{ but } \beta_{ep} \le 1 \tag{7}$$

$$N_{Ed}/N_{pl,Rd} + M_{Ed}/M_{ep,Rd} \le 1 \tag{8}$$

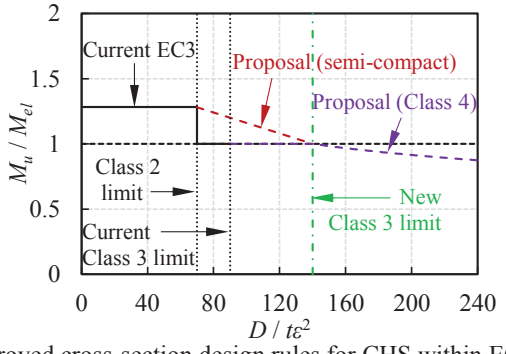

Figure 2. Improved cross-section design rules for CHS within EC3 framework.

4.2 *Assessment of design methods*

The current and improved EC3 design rules are assessed in this section using the generated FE data and the test results collected and reported by Meng and Gardner (submitted). The test and numerical ultimate loads are normalised by the predicted resistances and plotted in Figure 3 for isolated loading and Figure 4 for combined loading, with the statistical results reported in Table 2. The shortcomings in the current EC3 are clearly shown, which stem primarily from the

neglect of strain hardening for Class 1 and the neglect of partial plastification and overly strict slenderness limits for Class 3 CHS. The proposed design rules, on the other hand, significantly improve the accuracy for bending and combined loading in the semi-compact range, and provide essential design guidance for Class 4 CHS despite a reasonable level of conservatism.

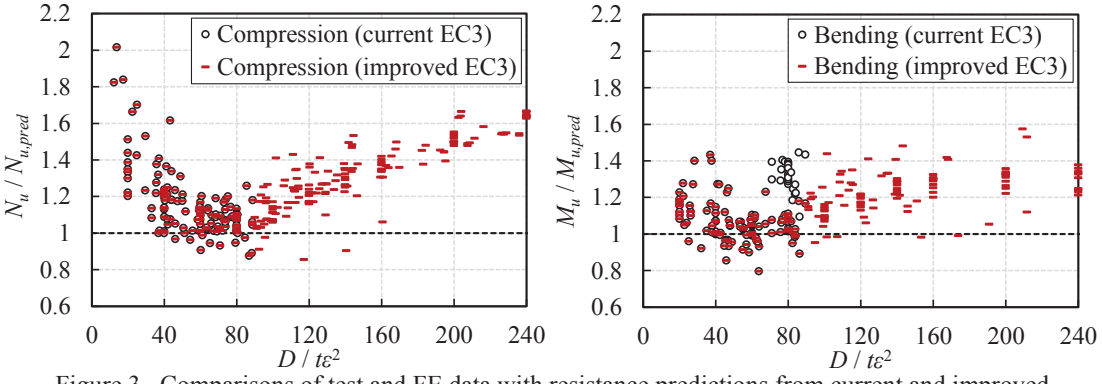

Figure 3. Comparisons of test and FE data with resistance predictions from current and improved (upcoming) EC3 for pure compression (left) and pure bending (right).

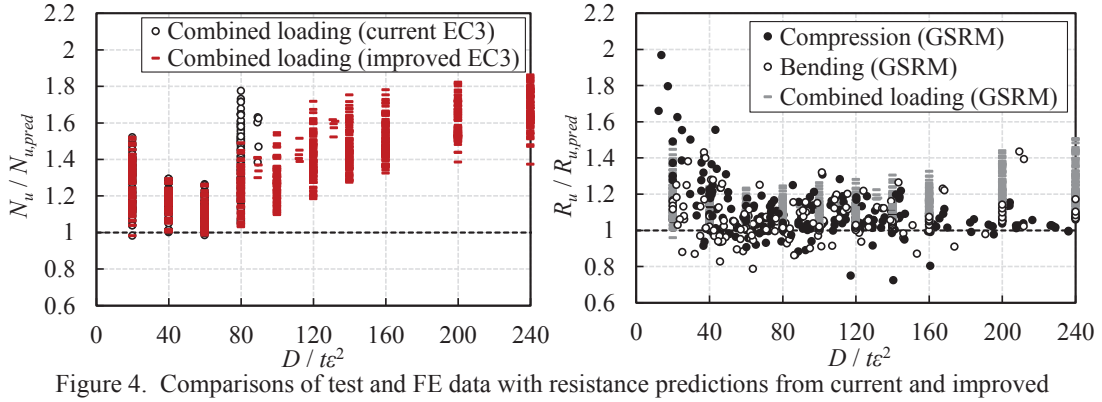

Figure 4. Comparisons of test and FE data with resistance predictions from current and improved (upcoming) EC3 for combined loading (left) and with resistance predictions from GSRM/CSM (right)

Table 2. Statistical results for test and FE resistances over design predictions

	Class 1 & 2		Class 3		Class 4	
	Mean	COV	Mean	COV	Mean	COV
Current EC3	1.157	0.125	1.360	0.134	-	
Improved EC3	-		1.257	0.110	1.459	0.130
New CSM	1.143	0.117	1.087	0.070	1.112	0.086

5 Generalised Slenderness-Based Resistance Method for CHS

A new generalised slenderness-based resistance method (GSRM) for CHS is developed utilising the CSM and is presented in this section. The key features of the proposal include: (i) reference resistances under combined loading, (i) relaxed Class 3 slenderness limits, (ii) re-calibrated base curves and (iv) new resistance functions based on the reference resistances. The accuracy of the proposed GSRM/CSM for CHS is assessed in Section 5.2.

5.1 *Design proposal*

The reference resistance R is defined as the load amplification factor with respect to the applied loads N_{Ed} and M_{Ed} to reach a certain limiting state. Three R factors – R_{el}, R_{pl} and $R_{cr,L}$, which represent the load amplification factors to reach the elastic, fully plastic and elastic critical local buckling resistances respectively, are used herein; their values were calculated using dedicated numerical tools in the present study. The generalised local slenderness $\bar{\lambda}_L$ based on the R factors is defined by Eq. (9), which is equivalent to the definition of the local slenderness in the current CSM. By substituting the theoretical equation for the elastic critical buckling stress $\sigma_{cr} = (E/\sqrt{3(1-\nu^2)})(2t/D)$, where ν is the Poisson's ratio, into $\bar{\lambda}_L$, the relationship between the EC3 local slenderness $D/t\varepsilon^2$ and $\bar{\lambda}_L$ can then be established, as given by Eq. (9).

$$\bar{\lambda}_L = \sqrt{R_{el}/R_{cr,L}} = \sqrt{f_y/\sigma_{cr}} = 0.0304\sqrt{D/(t\varepsilon^2)} \tag{9}$$

The current nonslender/slender slenderness limits are examined herein. Through comparisons with the test data and the FE results in Figure 5, it is clearly revealed that the EC3 and current CSM limits are overly conservative for both compression and bending. Based on the trend of the test and FE data, new limits of $\bar{\lambda}_0 = 0.36$ (corresponding to $D/t\varepsilon^2 = 140$) for compression and $\bar{\lambda}_0 = 0.43$ (corresponding to $D/t\varepsilon^2 = 200$) for bending are proposed. For combined loading, a transition between the limits for compression and bending based on ψ is proposed, as given by Eq. (10).

$$\bar{\lambda}_0 = 0.43 - 0.07\left((1+\psi)/2\right)^2 \tag{10}$$

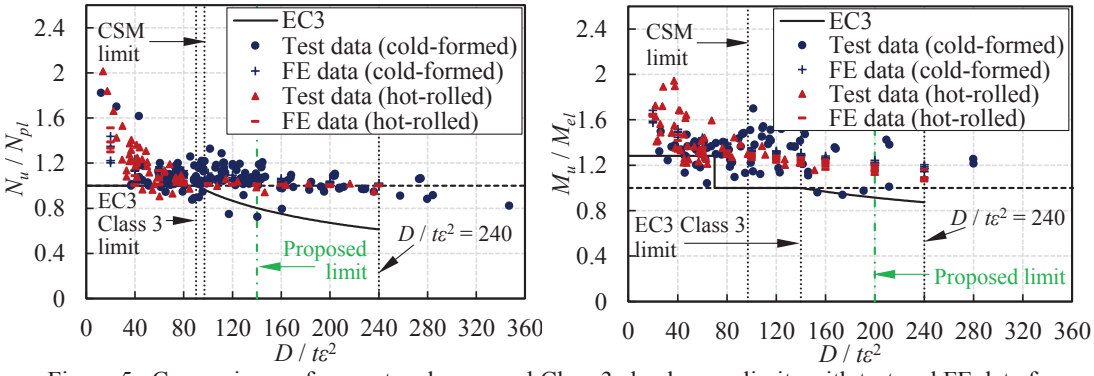

Figure 5. Comparisons of current and proposed Class 3 slenderness limits with test and FE data for compression (left) and bending (right).

The general form of the base curve is given by Eqs (11-12), where $A_1 = (1-\bar{\lambda}_0^{B_2})\bar{\lambda}_0^{B_2}$, B_1 and B_2 are the coefficients that describe the shape of the base curve, ε_u is the ultimate strain equal to the larger value of 0.06 and $0.6(1 - f_y/f_u)$ for hot-rolled and $0.6(1 - f_y/f_u)$ for cold-formed steels, C_1 is a material coefficient given by Eq. (13) for hot-rolled and 0.4 for cold-formed steels and ε_{sh} is the strain hardening strain for hot-rolled steels, as given by Eq. (14) (Yun et al. 2018, Yun and Gardner 2018). The current CSM base curve for CHS employs $\bar{\lambda}_0 = 0.3$, $B_1 = 4.5$ and $B_2 = 0.342$ for all loading scenarios (Buchanan et al. 2016), as plotted in Figure 6 along with the test data on CHS. New base curves, which employ the new slenderness limits in Eq. (10) and account for the different deformation capacities under different loading conditions, are developed herein. Based on the trend of the test data and calibration against the FE results,

$B_1 = 3.5$ for pure compression and 2.5 for pure bending, and $B_2 = 0.3$ for all load cases, are proposed; for combined loading, a transition for B_1 based on ψ – $B_1 = 2.5 + ((1+\psi)/2)^2$, is adopted. The proposed base curves are also plotted in Figure 6, where they can be seen to accurately capture the trend of the test data points.

$$\varepsilon_{csm}/\varepsilon_y = \left(\bar{\lambda}_0/\bar{\lambda}_L\right)^{B_1} \le \min\left(15, C_1\varepsilon_u/\varepsilon_y\right) \text{ for } \bar{\lambda}_L \le \bar{\lambda}_0 \tag{11}$$

$$\varepsilon_{csm}/\varepsilon_y = \left(1 - A_1/\bar{\lambda}_L^{B_2}\right)/\bar{\lambda}_L^{B_2} \text{ for } \bar{\lambda}_L > \bar{\lambda}_0 \tag{12}$$

$$C_1 = \left(\varepsilon_{sh} + 0.25\left(\varepsilon_u - \varepsilon_{sh}\right)\right)/\varepsilon_u \text{ for hot-rolled steels} \tag{13}$$

$$\varepsilon_{sh} = 0.1 f_y/f_u - 0.055 \text{ but } 0.015 \le \varepsilon_{sh} \le 0.03 \text{ for hot-rolled steels} \tag{14}$$

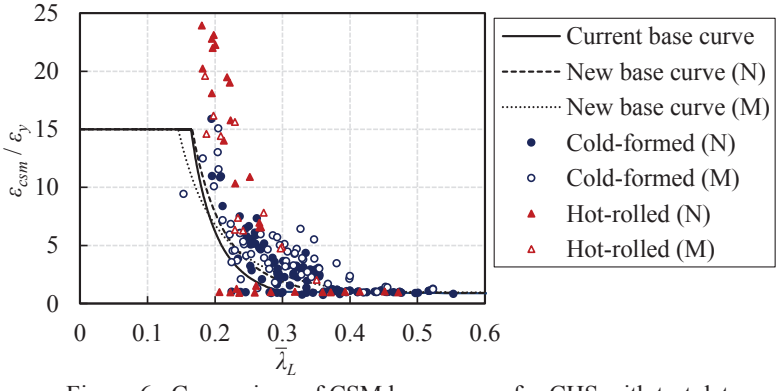

Figure 6. Comparison of CSM base curves for CHS with test data.

An elastic, linear hardening model for cold-formed (Yun and Gardner 2018) and a quad-linear model for hot-rolled steels (Yun et al. 2018), as those adopted in the current CSM, are also employed. New resistance functions based on the reference resistances are rationalised from the current CSM resistance functions. For stocky cold-formed CHS, a new resistance function – Eq. (15), which takes the form of the current CSM resistance function for bending (Yun and Gardner 2018), but with R_{pl} and R_{el} in place of W_{pl} and W_{el} respectively, is proposed for all load cases, where R_{csm} is the load amplification factor to reach the cross-section resistance and E_{sh} is the strain hardening slope, as defined by Yun et al. (2018) and Yun and Gardner (2018).

$$R_{csm} = R_{pl}\left(1 - \left(1 - \frac{R_{el}}{R_{pl}}\right)/\left(\frac{\varepsilon_{csm}}{\varepsilon_y}\right)^2 + \frac{E_{sh}}{E}\frac{R_{el}}{R_{pl}}\left(\frac{\varepsilon_{csm}}{\varepsilon_y} - 1\right)\right) \text{ for } \bar{\lambda}_L \le \bar{\lambda}_0 \tag{15}$$

For stocky hot-rolled CHS, new resistance functions – Eqs (16-17), which are modified similarly from the current CSM resistance functions for bending (Yun et al. 2018), are proposed.

$$R_{csm} = R_{pl}\left(1 - \left(1 - R_{el}/R_{pl}\right)/\left(\varepsilon_{csm}/\varepsilon_y\right)^2\right) \text{ for } \varepsilon_y < \varepsilon_{csm} \le \varepsilon_{sh} \tag{16}$$

$$R_{csm} = R_{pl}\left(1 - \left(1 - \frac{R_{el}}{R_{pl}}\right)/\left(\frac{\varepsilon_{csm}}{\varepsilon_y}\right)^2 + 0.1\left(\frac{\varepsilon_{csm} - \varepsilon_{sh}}{\varepsilon_y}\right)^2\frac{E_{sh}}{E}\right) \text{ for } \varepsilon_{csm} > \varepsilon_{sh} \tag{17}$$

For slender CHS, Eq. (18) is employed for both hot-rolled and cold-formed CHS.

$$R_{csm} = R_{el}\left(\varepsilon_{csm} / \varepsilon_{y}\right) \text{ for } \overline{\lambda}_0 < \overline{\lambda}_L \leq 0.6 \tag{18}$$

5.2 *Assessment of design methods*

The accuracy of the proposed new CSM for CHS is evaluated in this section. The test and FE results R_u are normalised by the predicted resistances $R_{u,pred}$ and plotted in Figure 4, from which significant improvements in both accuracy and consistency over EC3 (Figures 3 and 4) can be observed. The improvements are also shown quantitatively by the statistical results in Table 2.

6 Conclusions

A comprehensive study into the cross-sectional behaviour and design of CHS has been conducted. A numerical programme was initially conducted to expand the cross-section data pool on CHS. Improved design rules, including new slenderness limits, expressions for effective section properties and a new design approach for semi-compact CHS, along with a new generalised slenderness-based resistance method for CHS, were developed. Assessment of the design proposals was carried out using the numerical data and existing test results; significant improvements in accuracy over the current EC3 approach were demonstrated.

Acknowledgments

This study is part of the European project HOLLOSSTAB and was funded by the Research Fund for Coal and Steel (RFCS) under Grant Agreement No. 709892 (2016).

References

Abaqus 2016, *Abaqus 2016*, Dassault Systèmes, Simulia Corporation, United States, 2016.

Chan, T.M. and Gardner, L., Bending strength of hot-rolled elliptical hollow sections, *J. Constr. Steel Res.*, 64(9), 971-986, 2008a.

Chan, T.M. and Gardner, L., Compressive resistance of hot-rolled elliptical hollow sections, *Eng. Struct.*, 30(2), 522-532, 2008b.

Buchanan, C., Gardner, L. and Liew, A., The continuous strength method for the design of circular hollow sections, *J. Constr. Steel Res.*, 118, 207-216, March, 2016.

Gardner, L. and Yun, X., Description of stress-strain curves for cold-formed steels, *Constr. Build. Mater.*, 189, 527-538, November, 2018.

Meng, X. and Gardner, L., Cross-sectional behaviour of cold-formed high strength steel CHS under combined axial compression and bending, in *ICTWS 2018*, Lisbon, Portugal, 2018.

Meng, X. and Gardner, L., Elasto-plastic behaviour and design of semi-compact circular hollow sections, submitted.

Yun, X. and Gardner, L., Stress-strain curves for hot-rolled steels, *J. Constr. Steel Res.*, 133, 36-46, June, 2017.

Yun, X. and Gardner, L., The continuous strength method for the design of cold-formed steel non-slender tubular cross-sections, *Eng. Struct.*, 175, 549-564, November, 2018.

Yun, X., Gardner, L. and Boissonnade, N., The continuous strength method for the design of hot-rolled steel cross-sections, *Eng. Struct.*, 157, 179-191, February, 2018.